Asynchronous Control for Discrete-Time Markov Jump Systems with Multi-Node Round-Robin Protocol

Qi Fang, Lanlan He, Jie Liu, and Taiping Jiang

***Abstract*—This paper considers the asynchronous control for discrete-time Markov jump systems (MJSs) using a multi-node round-robin protocol (MNRRP). Compared to the traditional round-robin protocol, MNRRP increases the number of nodes updated at each transmission time, thereby improving system performance. In addition, a hidden Markov model is constructed to address the asynchronous behavior between the controlled object and the controller. Using Lyapunov functions and several inequalities, a criterion is provided to ensure the stochastic stability of MJS and joint $\mathcal{L}_2 - \mathcal{L}_\infty$ and $\mathcal{H}_\infty$ performance. A required asynchronous controller design approach is then presented based on the scheduling signal. Finally, a numerical example is given to verify the feasibility and applicability of the theoretical results.**

***Index Terms*—Markov jump system, hidden Markov model, round-robin protocol, asynchronous control**

I. Introduction

MARKOV jump systems (MJSs) are a class of stochastic hybrid systems capable of switching between different modes according to a Markov process. These systems can undergo random, abrupt changes in structure or parameters, with mode switching dictated by a Markov chain. This feature enables MJSs to model and analyze systems facing sudden disturbances, component failures, actuator repairs, and other abrupt structural variations effectively [1], [2]. Consequently, MJSs have found extensive applications in various practical scenarios, including traffic engineering [3], solar power plants [4], and the spread of infectious diseases [5]. Recently, substantial research progress has been made in such systems [6]–[11]. MJSs can generally be divided into two types: continuous-time MJSs [12] and discrete-time MJSs (DTMJSs) [13]. Unlike continuous-time MJSs, DTMJSs operate in discrete time steps, offering simpler analysis and implementation in digital systems. DTMJSs prove particularly useful in applications with observations and control actions naturally sampled at discrete intervals, such as digital signal processing and computer-based control systems.

Manuscript received July 19, 2024; revised November 29, 2024.

This work was supported by the Undergraduate Scientific Research Training Program of Anhui University of Technology (Grant No S202310360291).

Qi Fang is a postgraduate student at the School of Computer Science and Technology, Anhui University of Technology, Ma'anshan, 243032, China (email: fangqi202302@163.com)

Lanlan He is a postgraduate student at the School of Computer Science and Technology, Anhui University of Technology, Ma'anshan, 243032, China (email: hll20010118@163.com)

Jie Liu is an undergraduate student at the School of Computer Science and Technology, Anhui University of Technology, Ma'anshan, 243032, China (email: 1109279180@qq.com)

Taiping Jiang is an associate professor at the School of Computer Science and Technology, Anhui University of Technology, Ma'anshan, 243032, China (corresponding author, email: tpjiang2008@163.com)

Due to the limitations of bandwidth and data rates, only a limited number of signals can be transmitted simultaneously between system components [14], [15]. Therefore, effectively scheduling node access is crucial for conserving communication resources and preventing data congestion. Various scheduling protocols address these challenges, including the Round-Robin protocol (RRP), the weighted try-once-discard protocol, and the stochastic communication protocol [16]–[18]. Compared to other protocols, RRP [18] offers straightforward implementation, predictable scheduling, and fair resource allocation. However, traditional RRP [19]–[22] limits channel access to one node per transmission time, which, while reducing congestion, provides less information per transmission. In contrast, the multi-node Round-Robin protocol (MNRRP), which allows multiple nodes to transmit information simultaneously rather than a single node [23]–[26], has garnered increasing attention. This protocol was first proposed in [23] to address issues related to lossy networks with variable packet lengths. Subsequently, Hu et al. [24] investigated a network mode-dependent MNRRP for networked singularly perturbed systems with Markov lossy networks, Zhang et al. [25] focused on MNRRP for interval type-2 Takagi-Sugeno (T-S) fuzzy systems under probabilistic saturation constraints, and Song et al. [26] proposed a synthesis and analysis scheme for T-S aero-engine systems using the MNRRP to coordinate communication resources.

In practical scenarios, achieving comprehensive access to system modes proves challenging. In networked control systems, components are often geographically dispersed and communicate via unreliable channels, leading to discrepancies between received and original signals, mode mismatches, and asynchrony. Asynchronous controllers thus emerge as a pragmatic and increasingly researched solution. For instance, Zhou et al. [27] proposed a methodical two-step approach utilizing backtracking and optimization search for asynchronous quantized control of fuzzy MJSs within a networked control framework. Zhang et al. [28] examined the problem of secure asynchronous control of MJSs in the presence of non-periodic discrete denial of service attacks, while Tao et al. [29] addressed asynchronous $\mathcal{H}_\infty$ control issues in discrete-time hidden MJSs with complex mode transitions.

In the field of modern control theory, $\mathcal{H}_\infty$ control and $\mathcal{L}_2 - \mathcal{L}_\infty$ control are two significant control methodologies. $\mathcal{H}_\infty$ control primarily addresses the lower limit of L_2 gain, whereas $\mathcal{L}_2 - \mathcal{L}_\infty$ control aims to restrict peak energy gain to a specified threshold, thereby bolstering system robustness and curbing peak output [30], [31]. The joint use of $\mathcal{H}_\infty$ control with $\mathcal{L}_2-\mathcal{L}_\infty$ control effectively meets these dual objectives. Thus, the question arises: Can asynchronous control methods, combined with strategies like MNRRP, effectively handle the complexities of networked systems with mode mismatches and limited bandwidth while ensuring the joint performance of $\mathcal{L}_2-\mathcal{L}_\infty$ and $\mathcal{H}_\infty$ controls? This issue, to our knowledge, remains open and challenging, warranting further investigation.

Based on these insights, this paper studies the design problem of asynchronous control for DTMJSs using a MNRRP. In contrast to the traditional RRP, MNRRP updates multiple nodes at each transmission interval, which leads to improved system performance. A hidden Markov model (HMM) is constructed to account for the asynchronous behavior. A criterion is provided to ensure that the MJS is stochastically stable (SS) and joint $\mathcal{L}_2-\mathcal{L}_\infty$ and $\mathcal{H}_\infty$ performance. Subsequently, a token-based asynchronous state feedback control method is proposed. Finally, an example demonstrates the feasibility and applicability of the theoretical results.

Notation: Throughout, $\mathbb{R}^n$ refers to the n-dimensional Euclidean space, while $\mathbb{R}^{m\times n}$ denotes the set of all $m\times n$ real matrices. The notation $\mathrm{diag}\{\cdot\}$ is used to represent a block diagonal matrix, and $\mathbb{E}\{\cdot\}$ signifies the mathematical expectation. A real symmetric matrix $Q>0$ indicates that Q is positive definite.

II. Preliminaries

Consider a class of DTMJS described by:

$$\begin{cases} x(k+1)=A_{r_k}x(k)+B_{r_k}u(k)+D_{r_k}\omega(k), \\ \quad z(k)=C_{r_k}x(k), \end{cases} \tag{1}$$

where $x(k)\in\mathbb{R}^d$, $z(k)\in\mathbb{R}^{n_z}$, and $u(k)\in\mathbb{R}^{n_u}$ are the state vector, output vector, and control input, respectively. $\omega(k)\in\mathbb{R}^{n_w}$ describes the disturbance, taking values in $l_2[0,\infty)$. A_{r_k}, B_{r_k}, C_{r_k}, and D_{r_k} are pre-known system matrices, which depend on a discrete-time Markov chain (DTMC) $\{r_k, k\geq 0\}$ that takes values in a finite set $\mathcal{M}=\{1,2,\cdots,m\}$. The transition probability (TP) of system (1) is elicited as

$$\Pr\{r_{k+1}=s\,|\,r_k=i\}=\pi_{is}, \tag{2}$$

where $\pi_{is}\geq 0$, and $\sum_{s\in\mathcal{M}}\pi_{is}=1$, $\forall i,s\in\mathcal{M}$, and TP matrix $\Pi=[\pi_{is}]_{m\times m}$ [32].

To facilitate the discussion, $\forall i\in\mathcal{M}$, A_{r_k}, B_{r_k}, C_{r_k}, and D_{r_k} are denoted by A_i, B_i, C_i, and D_i, respectively.

The structure of system, as shown in Fig. 1, illustrates the utilization of a MNRRP to coordinate the transmission of d actuator nodes. In contrast to traditional RRPs, which only allow one actuator node to access the network at any given time, the MNRRP adopted in this study enables multiple consecutive actuators' measurement signals to be encapsulated into a single data packet transmission within a limited-bandwidth channel. This approach holds the potential to enhance system performance, with scheduling rules outlined in (3) and (4). The parameter $l(1\leq l\leq d)$, representing the number of selected actuators, is referred to as the packet length. Subsequently, the buffer is defined later.

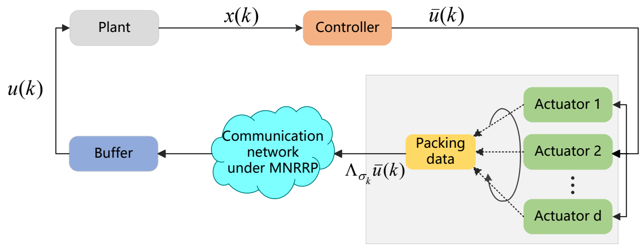

Fig. 1. The structure of the system with communication network.

Let $\varrho_k\in\mathcal{D}$, where $\mathcal{D}=\{1,2,\cdots,d\}$, be referred to as the token, representing the first of the l selected access actuator nodes at the current instant. The updating rule is as follows:

$$\varrho_k=\begin{cases}1, & k=1,\\ \mathrm{mod}(\varrho_{k-1}+l-1,d)+1, & k\geq 2,\end{cases} \tag{3}$$

and $\tilde{\varrho}_{q,k}$ $(q=1,\cdots,l)$ denotes all selected nodes as:

$$\tilde{\varrho}_{q,k}=\begin{cases}\varrho_k, & q=1,\\ \mathrm{mod}(\tilde{\varrho}_{q-1,k},d)+1, & q=2,\cdots,l.\end{cases} \tag{4}$$

Remark 1. The MNRRP evidently reduces to the standard RRP when $l=1$. Under this condition, $\varrho_k=\tilde{\varrho}_k=\mathrm{mod}(k-1,d)+1$. Moreover, in the MNRRP, the token ϱ_k is determined by both the time sequence k and the preceding token ϱ_{k-1}.

As described by the rules of MNRRP in (3) and (4), the actuator can access the value $\bar{u}_\nu(k)$ from the ν-th controller node if the node is selected and its data packet is transmitted successfully. Conversely, if the node is not selected or its data packet transmission fails, the actuator may rely on the previously received value. Consequently, the control signal available from the ν-th controller node to the actuator is defined as follows:

$$u_\nu(k)=\begin{cases}\bar{u}_\nu(k), & \lambda_{\nu,\varrho_k}=1,\\ u_\nu(k-1), & \text{otherwise}\end{cases} \tag{5}$$

with the index signal $\lambda_{\nu,\varrho_k}=1$ if $\tilde{\varrho}_{q,k}=\nu$ exists, and $\lambda_{\nu,\varrho_k}=0$ otherwise. Consequently, a concise expression for the compensator (5) can be formulated as follows:

$$u(k)=\Lambda_{\varrho_k}\bar{u}(k)+(I-\Lambda_{\varrho_k})u(k-1) \tag{6}$$

with $u(k)\triangleq[u_1^T(k),u_2^T(k),\cdots,u_d^T(k)]^T$ and $\Lambda_{\varrho_k}\triangleq\mathrm{diag}\{\lambda_{1,\varrho_k},\lambda_{2,\varrho_k},\cdots,\lambda_{d,\varrho_k}\}$.

In many cases, acquiring system mode information, represented by the DTMC r_k, is challenging due to various factors. To address this issue, a mode-dependent detector is employed, producing a stochastic process denoted as θ_k. Importantly, the stochastic process θ_k operates asynchronously with r_k. As in [33]–[36], a HMM is introduced to capture and model these asynchronous phenomena. For any $i\in\mathcal{M}$ and $j\in\mathcal{N}=\{1,2,\cdots,n\}$, the conditional probability matrix $\Omega=[\mu_{ij}]_{m\times n}$ is derived

$$\Pr\{\theta_k=j\,|\,r_k=i\}=\mu_{ij}, \tag{7}$$

where $\mu_{ij}\in[0,1]$ and $\sum_{j\in\mathcal{N}}\mu_{ij}=1$.

Next, an asynchronous controller is constructed as follows:

$$\bar{u}(k) = K_{\theta_k,\varrho_k}x(k), \tag{8}$$

where K_{θ_k,ϱ_k} represents the controller gains to be solved.

For $r_k = i$, $\theta_k = j$, and $\varrho_k = h$, the overall system (9) can be derived:

$$\begin{cases} x(k+1) = \bar{A}_{ijh}x(k) + \bar{B}_{ih}u(k-1) + D_i\omega(k), \\ \quad z(k) = C_ix(k), \end{cases} \tag{9}$$

where

$$\bar{A}_{ijh} = A_i + B_i\Lambda_hK_{jh},\ \bar{B}_{ih} = B_i(I-\Lambda_h).$$

Below, we provide the relevant definitions for system (9).

Definition 1. System (9) is said to be SS if for $\omega(k) = 0$, $u(-1) = 0$, and any initial condition (x_0, ϱ_0), it holds that

$$\mathbb{E}\left\{\sum_{k=0}^{\infty}\|x(k)\|^2 \,\middle|\, x_0, \varrho_0\right\} < \infty.$$

Definition 2. For a prescribed constant $\gamma > 0$, if, under the condition $x(0) = 0$,

$$\sup_{k\geq 0}\mathbb{E}\left\{z^T(k)z(k)\right\} \leq \gamma^2\sum_{k=0}^{\infty}w^T(k)w(k)$$

holds for all $w(k) \in l_2[0,\infty)$. Then, it can be said that system (9) has an $\mathcal{L}_2 - \mathcal{L}_\infty$ performance.

Definition 3. For a prescribed constant $\gamma > 0$, if, under the condition $x(0) = 0$,

$$\sum_{k=0}^{\infty}\mathbb{E}\left\{z^T(k)z(k)\right\} \leq \gamma^2\sum_{k=0}^{\infty}w^T(k)w(k)$$

holds for all $w(k) \in l_2[0,\infty)$. Then, it can be said that system (9) has an $\mathcal{H}_\infty$ performance.

Lemma 1. [37] Given a matrix $G = \begin{bmatrix} G_{11} & G_{12} \\ G_{12}^T & G_{22}\end{bmatrix}$, where $G_{11} \in \mathbb{R}^{r\times r}$, the following three conditions are equivalent:

(1) $G < 0$;
(2) $G_{11} < 0$, $G_{22} - G_{12}^TG_{11}^{-1}G_{12} < 0$;
(3) $G_{22} < 0$, $G_{11} - G_{12}G_{22}^{-1}G_{12}^T < 0$.

Lemma 2. [38] For any pair of matrices Y_1 and Y_2 that are positive definite and have compatible dimensions, the following inequality is valid:

$$-Y_1^TY_2^{-1}Y_1 \leq Y_2 - Y_1^T - Y_1.$$

Now we are in a position to state the purpose of this work explicitly: we intend to devise an asynchronous controller for DTMJSs. Our goal is to ensure that the resulting closed-loop system is SS and achieves joint $\mathcal{L}_2 - \mathcal{L}_\infty$ and $\mathcal{H}_\infty$ performance, while effectively using MNRRP to handle data collisions and congestion in a shared network environment.

III. Main Results

Lemma 3. The system (9) is SS, if there exist matrices $P_{ih} > 0$, $Q_{ih} > 0$, $R_{ij} > 0$, and K_{jh}, for $i \in \mathcal{M}$, $j \in \mathcal{N}$, and $h \in \mathcal{D}$ such that the following conditions hold:

$$\sum_{j=1}^{n}\mu_{ij}R_{ij} - P_{ih} < 0, \tag{10}$$

$$\begin{bmatrix} -\bar{P}_{s\epsilon}^{-1} & 0 & \bar{A}_{ijh} & \bar{B}_{ih} \\ 0 & -\bar{Q}_{s\epsilon}^{-1} & \Lambda_hK_{jh} & I-\Lambda_h \\ \bar{A}_{ijh}^T & K_{jh}^T\Lambda_h & -R_{ij} & 0 \\ \bar{B}_{ih}^T & I-\Lambda_h & 0 & -Q_{ih}\end{bmatrix} < 0, \tag{11}$$

where $\bar{P}_{s\epsilon} = \sum_{s=1}^{m}\pi_{is}P_{s\epsilon}$, $\bar{Q}_{s\epsilon} = \sum_{s=1}^{m}\pi_{is}Q_{s\epsilon}$.

Proof: Consider a mode-dependent Lyapunov function

$$V(k) = x^T(k)P_{ih}x(k) + u^T(k-1)Q_{ih}u(k-1), \tag{12}$$

and make the forward difference operator of (12) as

$$\begin{aligned} \Delta V(k) =& x^T(k+1)P_{s\epsilon}x(k+1) + u^T(k)Q_{s\epsilon}u(k) \\ &- x^T(k)P_{ih}x(k) - u^T(k-1)Q_{ih}u(k-1) \\ =& (\bar{A}_{ijh}x(k) + \bar{B}_{ih}u(k-1) + D_iw(k))^TP_{s\epsilon} \\ &\times (\bar{A}_{ijh}x(k) + \bar{B}_{ih}u(k-1) + D_iw(k)) \\ &+ (\Lambda_hK_{jh}x(k) + (I-\Lambda_h)u(k-1))^TQ_{s\epsilon} \\ &\times (\Lambda_hK_{jh}x(k) + (I-\Lambda_h)u(k-1)) \\ &- x^T(k)P_{ih}x(k) - u^T(k-1)Q_{ih}u(k-1), \end{aligned}$$

where $\epsilon = \sigma_{k+1}$. Let $w(k) = 0$ and perform the expectation operation on $\Delta V(k)$, we obtain

$$\begin{aligned} \mathbb{E}\{\Delta V(k)\} =& \mathbb{E}\{\eta^T(k)\sum_{j=1}^{n}\mu_{ij}(\Psi_1^T\bar{P}_{s\epsilon}\Psi_1 + \Psi_2^T\bar{Q}_{s\epsilon}\Psi_2 \\ &- \check{I})\eta(k) - x^T(k)P_{ih}x(k)\}, \end{aligned} \tag{13}$$

where $\eta(k) = \text{col}\{x(k), u(k-1)\}$, $\Psi_1 = \begin{bmatrix}\bar{A}_{ijh} & \bar{B}_{ih}\end{bmatrix}$, $\Psi_2 = \begin{bmatrix}\Lambda_hK_{jh} & I-\Lambda_h\end{bmatrix}$, $\check{I} = \text{diag}\{0, Q_{ih}\}$. By applying Lemma 1, we can derive from (11) that

$$\Psi_1^T\bar{P}_{s\epsilon}\Psi_1 + \Psi_2^T\bar{Q}_{s\epsilon}\Psi_2 - \check{I} < \check{R}_{ij}, \tag{14}$$

where $\check{R}_{ij} = \text{diag}\{R_{ij}, 0\}$. Substituting (14) into (13), we get

$$\begin{aligned} \mathbb{E}\{\Delta V(k)\} <& \mathbb{E}\left\{\eta^T(k)\sum_{j=1}^{n}\mu_{ij}\check{R}_{ij}\eta(k) - x^T(k)P_{ih}x(k)\right\} \\ =& \mathbb{E}\left\{x^T(k)\left(\sum_{j=1}^{n}\mu_{ij}R_{ij} - P_{ih}\right)x(k)\right\}. \end{aligned} \tag{15}$$

Therefore we can see from (10) that $\mathbb{E}\{\Delta V(k)\} < 0$. Let χ be the minimum eigenvalue of $-(\sum_{j=1}^{n}\mu_{ij}R_{ij} - P_{ih})$. then

$$\begin{aligned} \mathbb{E}\{V(\infty) - V(0)\} =& \mathbb{E}\left\{\sum_{k=0}^{\infty}\Delta V(k)\right\} \\ \leq& \mathbb{E}\left\{\sum_{k=0}^{\infty}(-\chi x^T(k)x(k))\right\}. \end{aligned} \tag{16}$$

Hence, we can get

$$\begin{aligned} \mathbb{E}\left\{\sum_{k=0}^{\infty}(x^T(k)x(k))\right\} \leq& \left\{\frac{1}{\chi}\{\mathbb{E}\{V(0)\} - \mathbb{E}\{V(\infty)\}\}\right\} \\ \leq& \frac{1}{\chi}\mathbb{E}\{V(0)\} \\ <& \infty. \end{aligned} \tag{17}$$

According to Definition 1, the system (9) is SS. ■

Below, we conduct a joint $\mathcal{L}_2 - \mathcal{L}_\infty$ and $\mathcal{H}_\infty$ performance analysis on system (9) and can give a criterion as follows:

Theorem 1. Given a positive constant $\gamma > 0$, the system (9) is SS and has a joint $\mathcal{L}_2 - \mathcal{L}_\infty$ and $\mathcal{H}_\infty$ performance guarantee, if there exist matrices $P_{ih} > 0$, $Q_{ih} > 0$, $R_{ij} > 0$, and K_{jh} such that the following conditions hold:

$$\sum_{j=1}^{n} \mu_{ij} R_{ij} - P_{ih} < 0, \tag{18}$$

$$\begin{bmatrix} -P_{ih} & C_i^T \\ C_i & -I \end{bmatrix} < 0, \tag{19}$$

$$\begin{bmatrix} \Theta_{ijh}^{11} & \Theta_{ijh}^{13} & \Theta_{ijh}^{14} \\ (\Theta_{ijh}^{13})^T & -\hat{Q}_{s\epsilon} & 0 \\ (\Theta_{ijh}^{14})^T & 0 & -\hat{P}_{s\epsilon} \end{bmatrix} < 0, \tag{20}$$

$$\begin{bmatrix} \Theta_{ijh}^{11} & \Theta_{i}^{12} & \Theta_{ijh}^{13} & \Theta_{ijh}^{14} \\ (\Theta_{i}^{12})^T & -I & 0 & 0 \\ (\Theta_{ijh}^{13})^T & 0 & -\hat{Q}_{s\epsilon} & 0 \\ (\Theta_{ijh}^{14})^T & 0 & 0 & -\hat{P}_{s\epsilon} \end{bmatrix} < 0, \tag{21}$$

where

$$\begin{aligned}
\Theta_{ijh}^{11} &= \mathrm{diag}\left\{-R_{ij}, -Q_{ih}, -\gamma^2 I\right\}, \\
\Theta_{i}^{12} &= \begin{bmatrix} C_i & 0 & 0 \end{bmatrix}^T, \\
\Theta_{ijh}^{13} &= \begin{bmatrix} \sqrt{\pi_{i1}} U_{jh}^T & \sqrt{\pi_{i2}} U_{jh}^T & \cdots & \sqrt{\pi_{im}} U_{jh}^T \end{bmatrix}, \\
\Theta_{ijh}^{14} &= \begin{bmatrix} \sqrt{\pi_{i1}} U_{ijh}^T & \sqrt{\pi_{i2}} U_{ijh}^T & \cdots & \sqrt{\pi_{im}} U_{ijh}^T \end{bmatrix}, \\
U_{jh} &= \begin{bmatrix} \Lambda_h K_{jh} & I - \Lambda_h & 0 \end{bmatrix}, \\
U_{ijh} &= \begin{bmatrix} \bar{A}_{ijh} & \bar{B}_{ih} & D_i \end{bmatrix}, \\
\hat{P}_{s\epsilon} &= \mathrm{diag}\left\{\tilde{P}_{1\epsilon}, \tilde{P}_{2\epsilon}, \cdots, \tilde{P}_{m\epsilon}\right\}, \\
\hat{Q}_{s\epsilon} &= \mathrm{diag}\left\{\tilde{Q}_{1\epsilon}, \tilde{Q}_{2\epsilon}, \cdots, \tilde{Q}_{m\epsilon}\right\}, \\
\tilde{P}_{s\epsilon} &= P_{s\epsilon}^{-1},\ \tilde{Q}_{s\epsilon} = Q_{s\epsilon}^{-1}.
\end{aligned}$$

Proof: Obviously, conditions (18) and (20) imply conditions (10) and (11), respectively. Therefore, in the case when $w(k) = 0$, system (9) is SS according to Lemma 3. Next, let us show that under the zero-initial condition, system (9) has a joint $\mathcal{L}_2 - \mathcal{L}_\infty$ and $\mathcal{H}_\infty$ performance. For any nonzero $w(k) \in l_2[0, \infty)$, define

$$\mathbb{J}_\alpha(k) = \gamma^2 w^T(k) w(k) + \mathbb{E}\left\{z^T(k) Z_\alpha z(k)\right\}, \tag{22}$$

where $\alpha \in \{1, 2\}$, $Z_1 = 0$, $Z_2 = -I$. Then, since $V(k) \geq 0$, we can deduce that

$$\begin{aligned}
&\mathbb{E}\left\{\Delta V(k)\right\} - \mathbb{J}_\alpha(k) \\
&= \mathbb{E}\{\sum_{j=1}^{n} \mu_{ij} \bar{\eta}^T(k) \left(\bar{\Psi}_1^T \bar{P}_{s\epsilon} \bar{\Psi}_1 + \bar{\Psi}_2^T \bar{Q}_{s\epsilon} \bar{\Psi}_2\right) \bar{\eta}(k) \\
&\quad - x^T(k) P_{ih} x(k) - u^T(k-1) Q_{ih} u(k-1)\} \\
&\quad - \gamma^2 w^T(k) w(k) - \mathbb{E}\left\{z^T(k) Z_\alpha z(k)\right\} \\
&= \mathbb{E}\{\sum_{j=1}^{n} \mu_{ij} \bar{\eta}^T(k) \left(\bar{\Psi}_1^T \bar{P}_{s\epsilon} \bar{\Psi}_1 + \bar{\Psi}_2^T \bar{Q}_{s\epsilon} \bar{\Psi}_2\right. \\
&\quad \left. - \bar{\Psi}_3^T Z_\alpha \bar{\Psi}_3 - \bar{I}\right) \bar{\eta}(k) - x^T(k) P_{ih} x(k)\},
\end{aligned} \tag{23}$$

where $\bar{\Psi}_1 = \begin{bmatrix} \bar{A}_{ijh} & \bar{B}_{ij} & D_i \end{bmatrix}$, $\bar{\Psi}_2 = \begin{bmatrix} \Lambda_h K_{jh} & I - \Lambda_h & 0 \end{bmatrix}$, $\bar{\Psi}_3 = \begin{bmatrix} C_i & 0 & 0 \end{bmatrix}$, $\bar{I} = \mathrm{diag}\left\{0, Q_{ih}, \gamma^2 I\right\}$, $\bar{\eta}(k) = \mathrm{col}\{x(k), u(k-1), w(k)\}$.

Case I: $\alpha = 1, Z_1 = 0$

According to (23), we obtain that

$$\begin{aligned}
&\mathbb{E}\left\{\Delta V(k)\right\} - \mathbb{J}_1(k) \\
&= \mathbb{E}\{\sum_{j=1}^{n} \mu_{ij} \bar{\eta}^T(k) \left(\bar{\Psi}_1^T \bar{P}_{s\epsilon} \bar{\Psi}_1 + \bar{\Psi}_2^T \bar{Q}_{s\epsilon} \bar{\Psi}_2\right. \\
&\quad \left. - \bar{I}\right) \bar{\eta}(k) - x^T(k) P_{ih} x(k)\}.
\end{aligned} \tag{24}$$

Based on Lemma 1, we can infer from (20) that

$$\bar{\Psi}_1^T \bar{P}_{s\epsilon} \bar{\Psi}_1 + \bar{\Psi}_2^T \bar{Q}_{s\epsilon} \bar{\Psi}_2 - \bar{I} < \bar{R}_{ij}, \tag{25}$$

where $\bar{R}_{ij} = \mathrm{diag}\left\{R_{ij}, 0, 0\right\}$. Substituting (25) into (24), we get

$$\begin{aligned}
&\mathbb{E}\left\{\Delta V(k)\right\} - \mathbb{J}_1(k) \\
&< \mathbb{E}\left\{\bar{\eta}^T(k) \left(\sum_{j=1}^{n} \mu_{ij} \bar{R}_{ij}\right) \bar{\eta}(k) - x^T(k) P_{ih} x(k)\right\} \\
&= \mathbb{E}\left\{x^T(k) \left(\sum_{j=1}^{n} \mu_{ij} R_{ij} - P_{ih}\right) x(k)\right\}.
\end{aligned} \tag{26}$$

Therefore we can see from (18) and (26) that

$$\mathbb{E}\left\{\Delta V(k)\right\} - \mathbb{J}_1(k) < 0. \tag{27}$$

By (19), it yields that

$$\begin{aligned}
\mathbb{E}\left\{z^T(k) z(k)\right\} &= \mathbb{E}\left\{x^T(k) C_i^T C_i x(k)\right\} \\
&\leq \mathbb{E}\left\{x^T(k) P_{ih} x(k)\right\} \\
&\leq \mathbb{E}\left\{V(k)\right\}.
\end{aligned} \tag{28}$$

And then, we continue to draw

$$\begin{aligned}
\mathbb{E}\left\{V(k)\right\} &= \mathbb{E}\left\{V(k) - V(0)\right\} \\
&= \sum_{\psi=0}^{k-1} \mathbb{E}\left\{\Delta V(\psi)\right\} \\
&\leq \sum_{\psi=0}^{k-1} \mathbb{E}\left\{\mathbb{J}_1(\psi)\right\}.
\end{aligned} \tag{29}$$

By means of (28) and (29), we can derive

$$\begin{aligned}
\mathbb{E}\left\{z^T(k) z(k)\right\} &\leq \sum_{\psi=0}^{k-1} \mathbb{E}\left\{\mathbb{J}_1(\psi)\right\} \\
&\leq \sum_{k=0}^{\infty} \mathbb{E}\left\{\mathbb{J}_1(k)\right\}.
\end{aligned} \tag{30}$$

In the light of (22), (30), and Definition 2, system (9) has the $\mathcal{L}_2 - \mathcal{L}_\infty$ performance.

Case II: $\alpha = 2, Z_2 = -I$

According to (23), we obtain that

$$\begin{aligned}
&\mathbb{E}\left\{\Delta V(k)\right\} - \mathbb{J}_2(k) \\
&= \mathbb{E}\{\sum_{j=1}^{n} \mu_{ij} \bar{\eta}^T(k) \left(\bar{\Psi}_1^T \bar{P}_{s\epsilon} \bar{\Psi}_1 + \bar{\Psi}_2^T \bar{Q}_{s\epsilon} \bar{\Psi}_2\right. \\
&\quad \left. + \bar{\Psi}_3^T I \bar{\Psi}_3 - \bar{I}\right) \bar{\eta}(k) - x^T(k) P_{ih} x(k)\}.
\end{aligned} \tag{31}$$

Utilizing Lemma 1, we can infer from (21) that

$$\bar{\Psi}_1^T \bar{P}_{s\epsilon} \bar{\Psi}_1 + \bar{\Psi}_2^T \bar{Q}_{s\epsilon} \bar{\Psi}_2 + \bar{\Psi}_3^T I \bar{\Psi}_3 - \bar{I} < \bar{R}_{ij}. \tag{32}$$

Substituting (32) into (31), we get

$$\begin{aligned}
&\mathbb{E}\left\{\Delta V(k)\right\} - \mathbb{J}_2(k) \\
&< \mathbb{E}\left\{\bar{\eta}^T(k) \left(\sum_{j=1}^{n} \mu_{ij} \bar{R}_{ij}\right) \bar{\eta}(k) - x^T(k) P_{ih} x(k)\right\}
\end{aligned}$$

$$= \mathbb{E}\left\{ x^T(k)\left(\sum_{j=1}^{n}\mu_{ij}R_{ij} - P_{ih}\right)x(k)\right\}. \tag{33}$$

Therefore we can see from (18) and (33) that

$$\mathbb{E}\{\Delta V(k)\} - \mathbb{J}_2(k) \le 0.$$

Further it can be concluded that,

$$\begin{aligned} -\mathbb{J}_2(k) &\le \mathbb{E}\{\Delta V(k)\} - \mathbb{J}_2(k) \\ &\le 0. \end{aligned} \tag{34}$$

Adding both sides of (34), we obtain

$$-\sum_{k=0}^{\infty}\mathbb{J}_2(k) \le 0. \tag{35}$$

In the light of (22), (35), and Definition 3, system (9) has the $\mathcal{H}_\infty$ performance.

Based on the above discussion, it can now be concluded that the system (9) has joint $\mathcal{L}_2 - \mathcal{L}_\infty$ and $\mathcal{H}_\infty$ performance, The proof is completed. ■

Building upon Theorem 1, we can develop a desired asynchronous controller design approach, described by the following theorem:

Theorem 2. Given a positive constant $\gamma > 0$, suppose that there exist matrices $\tilde{P}_{ih} > 0$, $\tilde{Q}_{ih} > 0$, $\tilde{R}_{ij} > 0$, N_{jh}, and $\tilde{K}_{jh}$, for $i \in \mathcal{M}$, $j \in \mathcal{N}$, and $h \in \mathcal{D}$ such that the following conditions hold:

$$\begin{bmatrix} -\tilde{P}_{ih} & \bar{\Gamma}_{ih} \\ \bar{\Gamma}_{ih}^T & -\Upsilon_i \end{bmatrix} < 0, \tag{36}$$

$$\begin{bmatrix} -\tilde{P}_{ih} & \tilde{P}_{ih}C_i^T \\ C_i\tilde{P}_{ih}^T & -I \end{bmatrix} < 0, \tag{37}$$

$$\begin{bmatrix} \bar{\Theta}_{ijh}^{11} & \bar{\Theta}_{ijh}^{13} & \bar{\Theta}_{ijh}^{14} \\ (\bar{\Theta}_{ijh}^{13})^T & -\hat{Q}_{s\epsilon} & 0 \\ (\bar{\Theta}_{ijh}^{14})^T & 0 & -\hat{P}_{s\epsilon} \end{bmatrix} < 0, \tag{38}$$

$$\begin{bmatrix} \bar{\Theta}_{ijh}^{11} & \bar{\Theta}_{ijh}^{12} & \bar{\Theta}_{ijh}^{13} & \bar{\Theta}_{ijh}^{14} \\ (\bar{\Theta}_{ijh}^{12})^T & -I & 0 & 0 \\ (\bar{\Theta}_{ijh}^{13})^T & 0 & -\hat{Q}_{s\epsilon} & 0 \\ (\bar{\Theta}_{ijh}^{14})^T & 0 & 0 & -\hat{P}_{s\epsilon} \end{bmatrix} < 0, \tag{39}$$

where

$$\begin{aligned}
\bar{\Gamma}_{ih} &= \begin{bmatrix} \sqrt{\mu_{i1}}\tilde{P}_{ih} & \sqrt{\mu_{i2}}\tilde{P}_{ih} & \cdots & \sqrt{\mu_{in}}\tilde{P}_{ih} \end{bmatrix}, \\
\Upsilon_i &= \mathrm{diag}\left\{\tilde{R}_{i1}, \tilde{R}_{i2}, \cdots, \tilde{R}_{in}\right\}, \\
\bar{\Theta}_{ijh}^{11} &= \mathrm{diag}\left\{\tilde{R}_{ij} - N_{jh}^T - N_{jh}, \tilde{Q}_{ih} - N_{jh}^T - N_{jh}, -\gamma^2 I\right\}, \\
\bar{\Theta}_{ijh}^{12} &= \begin{bmatrix} C_iN_{jh} & 0 & 0 \end{bmatrix}^T, \\
\bar{\Theta}_{ijh}^{13} &= \begin{bmatrix} \sqrt{\pi_{i1}}\bar{U}_{jh}^T & \sqrt{\pi_{i1}}\bar{U}_{jh}^T & \cdots & \sqrt{\pi_{im}}\bar{U}_{jh}^T \end{bmatrix}, \\
\bar{\Theta}_{ijh}^{14} &= \begin{bmatrix} \sqrt{\pi_{i1}}\bar{U}_{ijh}^T & \sqrt{\pi_{i1}}\bar{U}_{ijh}^T & \cdots & \sqrt{\pi_{im}}\bar{U}_{ijh}^T \end{bmatrix}, \\
\bar{U}_{jh} &= \begin{bmatrix} \Lambda_h\tilde{K}_{jh} & (I-\Lambda_h)N_{jh} & 0 \end{bmatrix}, \\
\bar{U}_{ijh} &= \begin{bmatrix} A_iN_{jh} + B_i\Lambda_h\tilde{K}_{jh} & B_i(I-\Lambda_h)N_{jh} & D_i \end{bmatrix}, \\
\tilde{P}_{ih} &= P_{ih}^{-1}, \ \tilde{R}_{ij} = R_{ij}^{-1}, \tilde{K}_{jh} = K_{jh}N_{jh}.
\end{aligned}$$

Then, the system (9) is SS and has a joint $\mathcal{L}_2 - \mathcal{L}_\infty$ and $\mathcal{H}_\infty$ performance guarantee. Additionally, if there are feasible solutions for (36)–(39), the controller gain K_{jh} can be determined using the following equation:

$$K_{jh} = \tilde{K}_{jh}N_{jh}^{-1}. \tag{40}$$

Proof: Here, nonlinear terms are dealt with by introducing slack matrices N_{jh}. Based on (38), we get the inequalities $\tilde{R}_{ij} - N_{jh}^T - N_{jh} < 0$ and $\tilde{Q}_{ij} - N_{jh}^T - N_{jh} < 0$. Thus, we can conclude that N_{jh} is positive definite, which guarantees that N_{jh} is invertible. Then, pre-multiplying and post-multiplying (36) by diag$\{P_{ih}, I\}$, we get

$$\begin{bmatrix} -P_{ih} & \Gamma_i \\ \Gamma_i^T & -\Upsilon_i \end{bmatrix} < 0, \tag{41}$$

where $\Gamma_i = \begin{bmatrix} \sqrt{\mu_{i1}}I & \sqrt{\mu_{i2}}I & \cdots & \sqrt{\mu_{in}}I \end{bmatrix}$. Applying Lemma 1 to (41), we get (18), thus showing that (18) can be guaranteed by (36). Similarly, (19) can be obtained by pre-multiplying and post-multiplying (37) by diag$\{P_{ih}, I\}$. The establishment of (19) is guaranteed by (37).

The next step is to verify the adequacy of (38) as a guarantee for the truth of (20). As stated in Lemma 2, we can infer the following inequality:

$$-N_{jh}^T\tilde{R}_{ij}^{-1}N_{jh} \le \tilde{R}_{ij} - N_{jh}^T - N_{jh}, \tag{42}$$

$$-N_{jh}^T\tilde{Q}_{ih}^{-1}N_{jh} \le \tilde{Q}_{ih} - N_{jh}^T - N_{jh}. \tag{43}$$

The results obtained from (38), (42), and (43) indicate that

$$\begin{bmatrix} \check{\Theta}_{ijh}^{11} & \bar{\Theta}_{ijh}^{13} & \bar{\Theta}_{ijh}^{14} \\ (\bar{\Theta}_{ijh}^{13})^T & -\hat{Q}_{s,\epsilon} & 0 \\ (\bar{\Theta}_{ijh}^{14})^T & 0 & -\hat{P}_{s,\epsilon} \end{bmatrix} < 0, \tag{44}$$

where $\check{\Theta}_{ijh}^{11} = \mathrm{diag}\{-N_{jh}^T\tilde{R}_{ij}^{-1}N_{jh}, -N_{jh}^T\tilde{Q}_{ih}^{-1}N_{jh}, -\gamma^2 I\}$.

And then, pre-multiplying and post-multiplying (44) by diag$\{(N_{jh}^T)^{-1}, (N_{jh}^T)^{-1}, I, \cdots, I\}$ and its transposed matrix, (44) is equivalent to (20). Similarly, the results obtained from (39), (42), and (43) indicate that

$$\begin{bmatrix} \check{\Theta}_{ijh}^{11} & \bar{\Theta}_{ijh}^{12} & \bar{\Theta}_{ijh}^{13} & \bar{\Theta}_{ijh}^{14} \\ (\bar{\Theta}_{ijh}^{12})^T & -I & 0 & 0 \\ (\bar{\Theta}_{ijh}^{13})^T & 0 & -\hat{Q}_{s,\epsilon} & 0 \\ (\bar{\Theta}_{ijh}^{14})^T & 0 & 0 & -\hat{P}_{s,\epsilon} \end{bmatrix} < 0. \tag{45}$$

And then, pre-multiplying and post-multiplying (45) by diag$\{(N_{jh}^T)^{-1}, (N_{jh}^T)^{-1}, I, \cdots, I\}$ and its transposed matrix, (45) is equivalent to (21). The proof is completed. ■

IV. Numerical Example

In this section, we will demonstrate the effectiveness of the designed controller by conducting relevant simulations. Assuming that the MJS model consists of two operating modes, the corresponding system matrices are shown as follows:

Mode 1:

$$A_1 = \begin{bmatrix} -0.36 & 0.15 & -0.67 \\ 0.35 & -0.50 & 0 \\ -0.89 & -0.39 & -0.28 \end{bmatrix}, B_1 = \begin{bmatrix} 0.22 & 0.2 & -0.3 \\ 0.01 & 0.22 & -0.06 \\ -0.3 & 0 & -0.09 \end{bmatrix},$$

$$C_1 = \begin{bmatrix} 0.4 & 0.1 & 0.1 \\ 0.2 & 0.5 & 0 \\ 0.1 & 0.11 & 0.2 \end{bmatrix}, D_1 = \begin{bmatrix} 0.15 & 0.2 & 0.1 \\ 0.2 & 0.14 & 0.12 \\ 0.2 & 0.13 & 0.11 \end{bmatrix}.$$

Mode 2:

$$A_2 = \begin{bmatrix} 0.95 & 0.22 & -0.04 \\ 0.22 & 0.39 & -0.14 \\ 0.07 & 0.20 & 0.10 \end{bmatrix}, B_2 = \begin{bmatrix} 0.16 & 0.1 & -0.01 \\ 0.02 & 0.32 & 0.01 \\ -0.11 & 0.14 & 0.13 \end{bmatrix},$$

$$C_2 = \begin{bmatrix} 0.16 & 0.1 & 0.17 \\ 0.2 & 0.1 & 0 \\ 0.1 & 0 & 0.11 \end{bmatrix}, D_2 = \begin{bmatrix} 0.15 & 0.15 & 0.05 \\ 0.03 & 0.13 & 0.03 \\ 0.12 & 0.22 & 0.23 \end{bmatrix}.$$

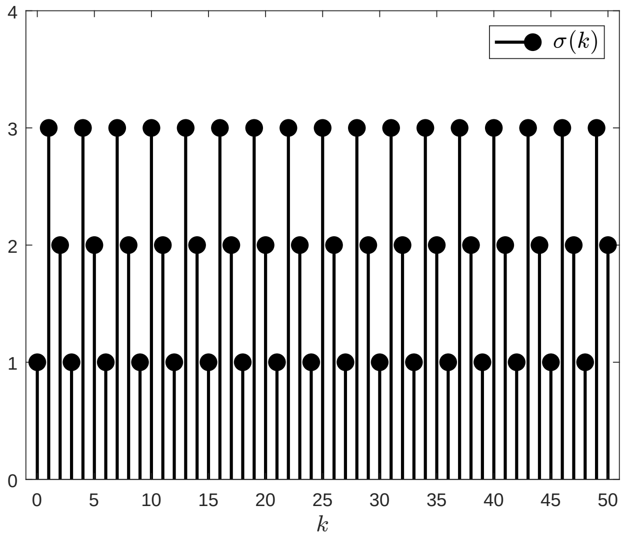

Fig. 2. Token selection situation.

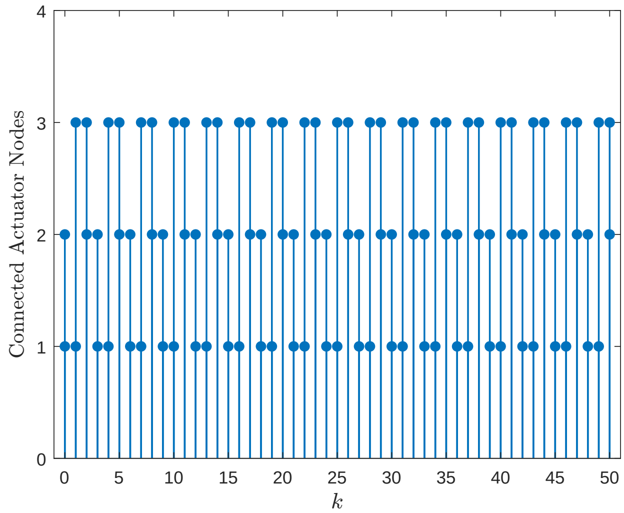

Fig. 3. Packet arrival condition.

The transitions of both the controlled system and the controller follow the TP matrix Π and the conditional probability matrix Ω as described below:

$$\Pi = \begin{bmatrix} 0.2 & 0.8 \\ 0.6 & 0.4 \end{bmatrix}, \Omega = \begin{bmatrix} 0.3 & 0.7 \\ 0.9 & 0.1 \end{bmatrix}.$$

Assume that the initial value of the scheduling signal ϱ_k is 1, and it is selected from 1 to 3 (as shown in Fig. 2). Let $l = 2$, meaning there are two nodes in the package, so there are always two executor nodes connected to the network at any moment (Fig. 3). Therefore, the three update matrices are respectively $\Lambda_1 = \text{diag}\{1, 1, 0\}$, $\Lambda_2 = \text{diag}\{0, 1, 1\}$, and $\Lambda_3 = \text{diag}\{1, 0, 1\}$. We further use the asynchronous controller design method proposed in Theorem 2 to obtain the following asynchronous controller gains:

$$K_{11} = \begin{bmatrix} 0.0000 & 0.0000 & 0.0000 \\ -0.2834 & -0.0807 & 0.3873 \\ 0 & 0 & 0 \end{bmatrix},$$

$$K_{12} = \begin{bmatrix} 0 & 0 & 0 \\ -0.1358 & 0.0264 & 0.1508 \\ 0.1787 & -0.0659 & -0.5134 \end{bmatrix},$$

$$K_{13} = \begin{bmatrix} -0.4783 & 0.0577 & 0.5567 \\ 0 & 0 & 0 \\ 0.0061 & -0.0409 & -0.0724 \end{bmatrix},$$

$$K_{21} = \begin{bmatrix} 0.0000 & 0.0000 & 0.0000 \\ -0.1629 & -0.0240 & 0.5876 \\ 0 & 0 & 0 \end{bmatrix},$$

$$K_{22} = \begin{bmatrix} 0 & 0 & 0 \\ -0.1049 & 0.1187 & 0.1829 \\ 0.0320 & -0.1898 & -0.4974 \end{bmatrix},$$

$$K_{23} = \begin{bmatrix} -0.2549 & 0.1445 & 0.5679 \\ 0 & 0 & 0 \\ -0.0008 & -0.0422 & -0.1635 \end{bmatrix}.$$

with the joint $\mathcal{L}_2 - \mathcal{L}_\infty$ and $\mathcal{H}_\infty$ performance index γ=1.4519. For comparison, we also consider a scenario where the network channel allows only one actuator node to exchange information at any given time, reducing the MNRRP to the simpler RRP case. Consequently, the update matrices change to $\Lambda_1 = \text{diag}\{1, 0, 0\}$, $\Lambda_2 = \text{diag}\{0, 1, 0\}$,

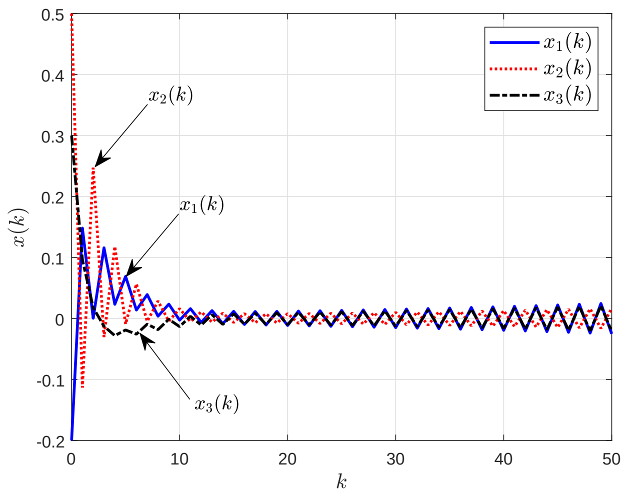

Fig. 4. State trajectories $x(k)$ of the open-loop system.

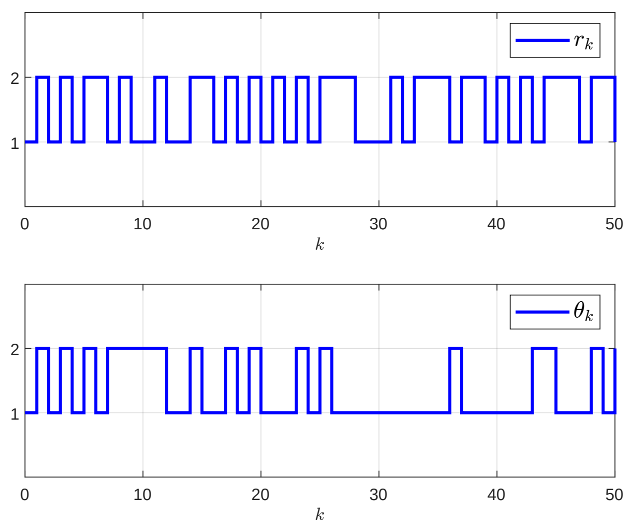

Fig. 5. Switching modes of the plant and controlle.

and $\Lambda_3 = \text{diag}\{0, 0, 1\}$. By applying the asynchronous controller design method described in Theorem 2, we can

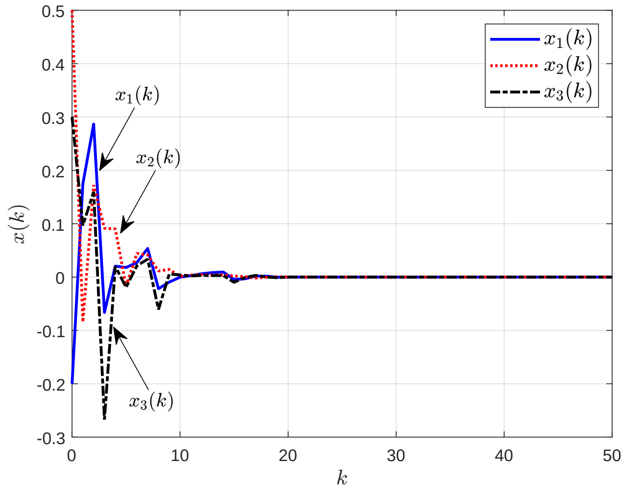

Fig. 6. State trajectories $x(k)$ of the closed-loop system.

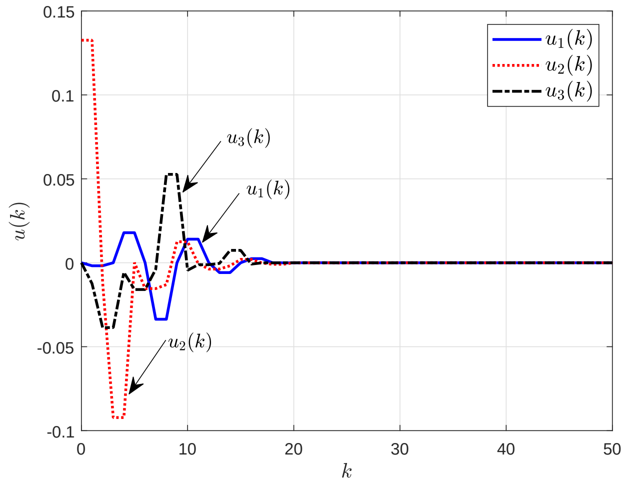

Fig. 7. Control input signals.

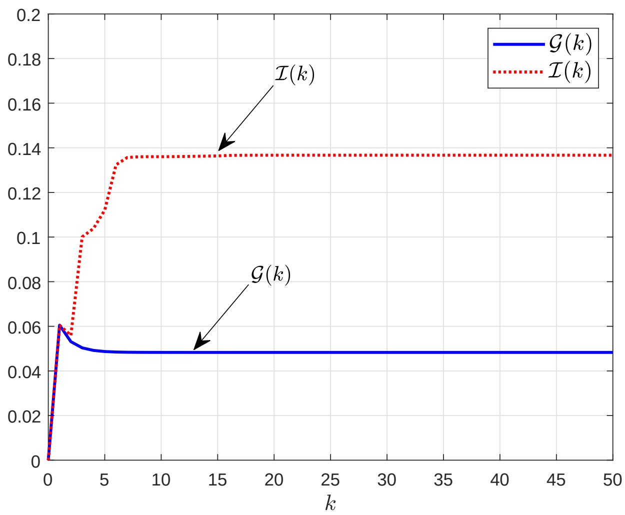

Fig. 8. The trajectories of $\mathcal{G}(k)$ and $\mathcal{I}(k)$.

obtain the corresponding asynchronous controller gains.

$$K_{11} = \begin{bmatrix} -0.0422 & 0.1222 & 0.0771 \\ 0 & 0 & 0 \\ 0 & 0 & 0 \end{bmatrix},$$

$$K_{12} = \begin{bmatrix} 0 & 0 & 0 \\ -0.0370 & -0.0891 & -0.0186 \\ 0 & 0 & 0 \end{bmatrix},$$

$$K_{13} = \begin{bmatrix} 0 & 0 & 0 \\ 0 & 0 & 0 \\ 0.1029 & -0.0263 & -0.2036 \end{bmatrix},$$

$$K_{21} = \begin{bmatrix} -0.0168 & 0.0824 & 0.0563 \\ 0 & 0 & 0 \\ 0 & 0 & 0 \end{bmatrix},$$

$$K_{22} = \begin{bmatrix} 0 & 0 & 0 \\ 0.0139 & -0.0943 & 0.0019 \\ 0 & 0 & 0 \end{bmatrix},$$

$$K_{23} = \begin{bmatrix} 0 & 0 & 0 \\ 0 & 0 & 0 \\ 0.0980 & -0.1284 & -0.2490 \end{bmatrix},$$

with the joint $\mathcal{L}_2 - \mathcal{L}_\infty$ and $\mathcal{H}_\infty$ performance index γ=2.3381.

Through a comparison of the two cases, we can conclude that the proposed control scheme under MNRRP enhances overall control performance.

Assume $x(0) = [-0.2 \quad 0.5 \quad 0.3]^T$ and $w(k) = e^{-0.4k}$. The state trajectories of the open-loop MJS are shown in Fig. 4. Fig. 5 depicts the resulting plant and controller modes. The evolution of the state $x(k)$ of the closed-loop system, according to the calculated asynchronous controller gains, is shown in Fig. 6, and the control signal is shown in Fig. 7. It can be concluded that the system (9) is stable.

We define

$$\mathcal{G}(k) = \frac{\sup_{k\geq 0} \mathbb{E}\{z^T(k)z(k)\}}{\sum_{k=0}^{\infty} w^T(k)w(k)},\ \mathcal{I}(k) = \frac{\sum_{k=0}^{\infty} \mathbb{E}\{z^T(k)z(k)\}}{\sum_{k=0}^{\infty} w^T(k)w(k)}.$$

Thus, the curves of $\mathcal{G}(k)$ and $\mathcal{I}(k)$ under zero initial condition are obtained (Fig. 8), and it is verified that $\mathcal{G}(\infty)$ and $\mathcal{I}(\infty)$ are less than $\gamma^2(= 2.1080)$. The simulation results illustrate the effectiveness of the proposed method.

V. Conclusion

This paper studied the problem of asynchronous control design for DTMJSs based on MNRRP. Compared to the traditional RRP, MNRRP updates several nodes at each transmission time, resulting in enhanced system performance. An HMM was constructed to address the asynchronous behavior between the plant and the controller. Using the Lyapunov functions and several inequalities, we established a criterion ensuring that the MJS is SS and has joint $\mathcal{L}_2 - \mathcal{L}_\infty$ and $\mathcal{H}_\infty$ performance. Subsequently, a required asynchronous controller design approach was presented based on the scheduling signal. Finally, a numerical example was used to verify the feasibility and effectiveness of the theoretical results.

References

[1] O. L. V. Costa, M. D. Fragoso, and R. P. Marques, *Discrete-Time Markov Jump Linear Systems*. Berlin: Springer, 2006.

[2] L. Zhang, T. Yang, P. Shi, Y. Zhu *et al.*, *Analysis and Design of Markov Jump Systems with Complex Transition Probabilities*. Cham, Switzerland: Springer, 2016.

[3] J. N. A. Bueno, L. B. Marcos, K. D. Rocha, and M. H. Terra, “Regulation of uncertain Markov jump linear systems with application on automotive powertrain control,” *IEEE Transactions on Systems, Man, and Cybernetics: Systems*, vol. 53, no. 8, pp. 5019–5031, 2023.

[4] R. H. M. Zargar and M. H. Y. Moghaddam, "Development of a Markov-chain-based solar generation model for smart microgrid energy management system," *IEEE Transactions on Sustainable Energy*, vol. 11, no. 2, pp. 736–745, 2020.
[5] F. Zuhairoh, D. Rosadi, and A. R. Effendie, "Continuous-time hybrid Markov/semi-Markov model with sojourn time approach in the spread of infectious diseases," *IAENG International Journal of Computer Science*, vol. 50, no. 3, pp. 1108–1114, 2023.
[6] E. K. Odorico, J. N. A. Bueno, and M. H. Terra, "Robust recursive regulator for polytopic Markovian jump linear systems with random state delays," *IEEE Transactions on Automatic Control, online, doi:10.1109/TAC.2024.3423568*, 2024.
[7] J. Zhou, J. Dong, S. Xu, and C. K. Ahn, "Input-to-state stabilization for Markov jump systems with dynamic quantization and multimode injection attacks," *IEEE Transactions on Systems, Man, and Cybernetics: Systems*, vol. 54, no. 4, pp. 2517–2529, 2024.
[8] J. Wu, G. Qin, J. Cheng, J. Cao, H. Yan, and I. Katib, "Adaptive neural network control for Markov jumping systems against deception attacks," *Neural Networks*, vol. 168, pp. 206–213, 2023.
[9] F. Xu and C. Wei, "Stability of nonlinear semi-Markovian switched stochastic systems with synchronously impulsive jumps driven by g-brownian motion," *IAENG International Journal of Computer Science*, vol. 50, no. 2, pp. 778–784, 2023.
[10] M. Fang, C. Zhou, X. Huang, X. Li, and J. Zhou, "$\mathcal{H}_\infty$ couple-group consensus of stochastic multi-agent systems with fixed and Markovian switching communication topologies," *Chinese Physics B*, vol. 28, no. 1, p. 010703, 2019.
[11] M. Sathishkumar, R. Sakthivel, C. Wang, B. Kaviarasan, and S. M. Anthoni, "Non-fragile filtering for singular Markovian jump systems with missing measurements," *Signal Processing*, vol. 142, pp. 125–136, 2018.
[12] L. He, X. Zhang, T. Jiang, and C. Tang, "Guaranteed performance control for delayed Markov jump neural networks with output quantization and data-injection attacks," *International Journal of Machine Learning and Cybernetics, online, doi:10.1007/s13042-024-02195-3*, 2024.
[13] M. K. Kumar, "Mixed $\mathcal{H}_\infty$ and passivity performance analysis of interfered digital filters with Markovian jumping parameters and delays," *Fluctuation and Noise Letters*, vol. 21, no. 01, p. 2250003, 2022.
[14] H. Zhao, D. Chen, and J. Hu, "Event-triggered nonfragile predictive control for networked control system with redundant channels," *Transactions of the Institute of Measurement and Control*, vol. 46, no. 1, pp. 58–69, 2024.
[15] Y. Tao, H. Tao, Z. Zhuang, V. Stojanovic, and W. Paszke, "Quantized iterative learning control of communication-constrained systems with encoding and decoding mechanism," *Transactions of the Institute of Measurement and Control*, vol. 46, no. 10, pp. 1943–1954, 2024.
[16] H. Liu, Z. Wang, W. Fei, and H. Dong, "On state estimation for discrete time-delayed memristive neural networks under the WTOD protocol: a resilient set-membership approach," *IEEE Transactions on Systems, Man, and Cybernetics: Systems*, vol. 52, no. 4, pp. 2145–2155, 2021.
[17] Y. Zhang, Y. Ji, T. Jiang, and J. Zhou, "Event-triggered control for roesser model-based 2D Markov jump systems under stochastic communication protocol," *Circuits, Systems, and Signal Processing*, vol. 43, no. 11, pp. 6953–6976, 2024.
[18] L. Zou, Z. Wang, Q.-L. Han, and D. Zhou, "Full information estimation for time-varying systems subject to round-robin scheduling: A recursive filter approach," *IEEE Transactions on Systems, Man, and Cybernetics: Systems*, vol. 51, no. 3, pp. 1904–1916, 2019.
[19] H. Shen, S. Huo, H. Yan, J. H. Park, and V. Sreeram, "Distributed dissipative state estimation for Markov jump genetic regulatory networks subject to round-robin scheduling," *IEEE Transactions on Neural Networks and Learning Systems*, vol. 31, no. 3, pp. 762–771, 2019.
[20] C. Gong, G. Zhu, P. Shi, and R. K. Agarwal, "Distributed fault detection and control for Markov jump systems over sensor networks with round-robin protocol," *IEEE Transactions on Circuits and Systems I: Regular Papers*, vol. 68, no. 8, pp. 3422–3435, 2021.
[21] H. Shang, G. Zong, and W. Qi, "Security control for networked discrete-time semi-Markov jump systems with round-robin protocol," *IEEE Transactions on Circuits and Systems II: Express Briefs*, vol. 69, no. 6, pp. 2812–2816, 2021.
[22] B. Li, Z. Wang, Q.-L. Han, and H. Liu, "Distributed quasiconsensus control for stochastic multiagent systems under round-robin protocol and uniform quantization," *IEEE Transactions on Cybernetics*, vol. 52, no. 7, pp. 6721–6732, 2020.
[23] J. Li, Y. Niu, and J. Song, "Sliding mode control design under multiple nodes round-robin-like protocol and packet length-dependent lossy network," *Automatica*, vol. 134, p. 109942, 2021.
[24] Y. Hu, O.-M. Kwon, C. Cai, and Y.-J. Kim, "Output feedback $\mathcal{H}_\infty$ control for discrete time singularly perturbed systems with Markov lossy network: the round-robin-like protocol case," *Applied Mathematics and Computation*, vol. 462, p. 128338, 2024.
[25] Z. Zhang and Y. Niu, "Probabilistic-constrained control of interval type-2 T-S fuzzy systems under the multi-node round-robin scheduling protocol," *Journal of the Franklin Institute*, vol. 360, no. 9, pp. 6566–6584, 2023.
[26] P. Song, Q. Yang, G. Wen, Z. Zhang, and J. Peng, "Fuzzy H_∞ robust control for TS aero-engine systems with network-induced factors under round-robin-like protocol," *Aerospace Science and Technology*, vol. 137, p. 108258, 2023.
[27] J. Zhou, J. Dong, and S. Xu, "Asynchronous dissipative control of discrete-time fuzzy Markov jump systems with dynamic state and input quantization," *IEEE Transactions on Fuzzy Systems*, vol. 31, no. 11, pp. 3906–3920, 2023.
[28] Y. Zhang and Z.-G. Wu, "Asynchronous control of Markov jump systems under aperiodic DoS attacks," *IEEE Transactions on Circuits and Systems II: Express Briefs*, vol. 70, no. 2, pp. 685–689, 2023.
[29] Y.-Y. Tao and Z.-G. Wu, "Optimal asynchronous control of discrete-time hidden Markov jump systems with complex transition probabilities," *IEEE Transactions on Systems, Man, and Cybernetics: Systems*, vol. 54, no. 2, pp. 1159–1167, 2024.
[30] Y. Wang, W. Hou, and J. Ding, "Robust control for a class of nonlinear switched systems with mixed delays," *Engineering Letters*, vol. 28, no. 3, pp. 903–911, 2020.
[31] L. Van Hien and N. T. Lan-Huong, "Observer-based $\mathcal{L}_2-\mathcal{L}_\infty$ control of 2D roesser systems with random packet dropout," *IET Control Theory & Applications*, vol. 14, no. 5, pp. 774–780, 2020.
[32] S. Purwani, R. A. M. Fasa, A. Tsanawafa, and S. Sutisna, "Long-term prediction of oil palm fresh fruit bunch prices in riau province post-pandemic using a discrete-time Markov chain," *IAENG International Journal of Applied Mathematics*, vol. 54, no. 6, pp. 1225–1232, 2024.
[33] X. Qin, J. Dong, X. Zhang, T. Jiang, and J. Zhou, "$\mathcal{H}_\infty$ control of time-delayed Markov jump systems subject to mismatched modes and interval conditional probabilities," *Arabian Journal for Science and Engineering*, vol. 49, no. 5, pp. 7471–7486, 2024.
[34] W.-J. Lin, Q. Wang, and G. Tan, "Asynchronous adaptive event-triggered fault detection for delayed Markov jump neural networks: A delay-variation-dependent approach," *Neural Networks*, vol. 171, pp. 53–60, 2024.
[35] X. Li, X. Ma, W. Tai, and J. Zhou, "Designing an event-triggered $\mathcal{H}_\infty$ filter with possibly inconsistent modes for Markov jump systems," *Digital Signal Processing*, vol. 139, p. 104092, 2023.
[36] S. Dong, L. Liu, G. Feng, M. Liu, Z.-G. Wu, and R. Zheng, "Cooperative output regulation quadratic control for discrete-time heterogeneous multiagent Markov jump systems," *IEEE Transactions on Cybernetics*, vol. 52, no. 9, pp. 9882–9892, 2022.
[37] S. Boyd, L. El Ghaoui, E. Feron, and V. Balakrishnan, *Linear Matrix Inequalities in System and Control Theory*. Philadelphia, USA: SIAM, 1994.
[38] E.-K. Boukas, *Control of singular systems with random abrupt changes*. Springer Science & Business Media, 2008.